Proceedings of the 28th IEEE
EMBS Annual International Conference
New York City, USA, Aug 30-Sept 3, 2006

Predicting Moment Arms in Diarthroidal Joints – 3D Computer Simulation Capability and Muscle-Tendon Model Validation

William L. Buford, Jr., *Member, IEEE*, Clark R. Andersen

***Abstract*— Interactive 3D simulation of musculoskeletal kinematics is used to predict the instantaneous moment arms of muscles acting about joints. Experimental studies were completed to verify the moment arms of muscles in the finger joints and at the knee. For other joints, predictions were compared with studies from the literature. Both methods provided for iterative improvement of the underlying 3D models of muscle tendon paths. Experimental results confirm that muscle-tendon moment arms vary throughout each joint's range-of-motion; most muscles have more than one function (affect more than one degree-of-freedom); and that computer simulation models can be improved through simple parametric changes in cubic B-spline models of muscle-tendon paths.**

I. Introduction

THIS report describes the use of interactive 3D computer graphic simulation of musculoskeletal kinematics in the generation (prediction) of muscle-tendon moment arms at joints; interactive use of the simulation to study the 3D balance of muscles at joints; design of experiments with fresh cadaver limbs to investigate the instantaneous moment arms of muscle-tendon units; improvement in the muscle-tendon path models integral to the simulation; and the iterative use of simulation and experiment resulting in improved understanding of musculoskeletal function. With real-time, interactive simulation musculoskeletal function is readily studied and predictions and hypotheses are rapidly generated. Thus the overall research cycle is enhanced as shown in Fig. 1.

Drawing on past experience using the simulation in knee, hand, and finger muscle mechanics, examples are presented to demonstrate this process [3, 4, 5, 12]. Typically, the simulation is used to generate questions regarding muscle balance and relative contribution to motion. Results from subsequent experimentation help to improve the simulation models, but most importantly help to clarify muscle-tendon-joint function in ways that have direct clinical impact.

Manuscript received March 30, 2006. This work was supported in part by the Texas Advanced Technology Program (Grant Number: 004952-0111-1999) and by a research grant from Smith Nephew, Inc. A portion of the simulation data structure developed in our work is from the National Library of Medicine Visible Human (male) frozen CT data set.

The authors are with the Department of Orthopaedic Surgery and Rehabilitation, University of Texas Medical Branch, 301 University Blvd, Galveston, TX 77555-0175 (corresponding author is William L. Buford, Jr., 409-747-3246; fax 409-747-3240; email: wbuford@utmb.edu).

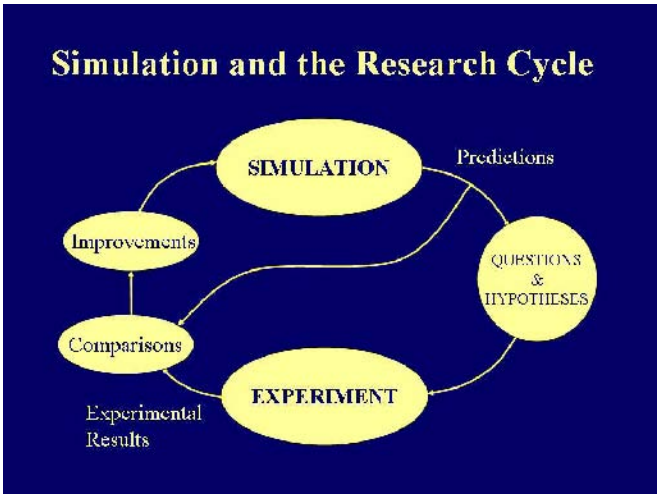

Fig. 1. The cycle of research with simulation in the loop. Interactive, real-time, 3D, computer graphic simulation of musculoskeletal kinematics provides acceleration to musculoskeletal research.

II. Material and Methods

A. Computer Simulation System

The simulation development environment is a dual 3.2 GHz Dual Pentium Xeon with Windows XP using Visual C++.NET, and OpenGL with the GLUT Library. The graphics driver is the Nvidia Quadro FX4000 256Mb graphics processor. In addition to mouse and keyboard interactive methods, this system utilizes pop-up menus with control widgets and 6 DOF control using a Spaceball (Spaceball model 5000, Spacetec IMC Corp., Lowell, MA). Use of the system for simulation of the extremities is described in [4].

The simulation upper and lower extremities were derived from a fresh cadaver (28 yr old male) obtained through the Texas willed body program. The limbs were scanned on a General Electric Computerized Tomography scanner (GE Model 9800). One-mm thick CT slices spaced at 1 mm are used for the joint areas that require the greatest resolution. One mm thick slices spaced 5 mm apart were used for the mid shaft areas of bones. This approach helps to maintain highest detail in critical areas and save on structure size where such detail is not needed. Structures for the head, trunk and spine were derived from axial computerized tomography (CT) slices of the National Library of Medicine Visible Human (male). The frozen CT structure was used because the slices are spaced at one mm apart (maximum vertical resolution). All images were run through the MIMICS interactive software package that creates triangular polygons representing each bone. MAGICS software

(MIMICS and MAGICS are from Materialise, Inc) is used where required to edit and combine the polygonal files. Files (in .stl format) for each bone then serve as the base level structures in the OpenGL kinematic hierarchy. B-spline muscle models with a variety of blending functions were developed to describe muscle-tendon paths for all skeletal muscles of the body [3, 4] (Fig 2).

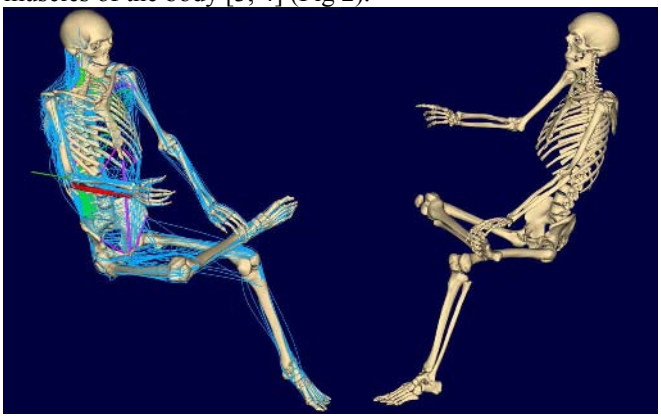

Fig. 2. Oblique views of the complete whole body simulation structure with muscle-tendon spline models included on the left. With the simulation, muscle moment arms at any joint can be studied during joint rotation in real-time. The simulation is built so that parameters within muscle definitions can be changed and resultant effects upon joint balance observed, also in real-time.

The ability to manually adjust and dynamically alter (with 6 DOF) effective axes of motion is provided within the kinematic structure. Up to three axes were defined at each articulation using interactive control with the Spaceball. Fig. 3 depicts all axes within the whole body structure. Initial

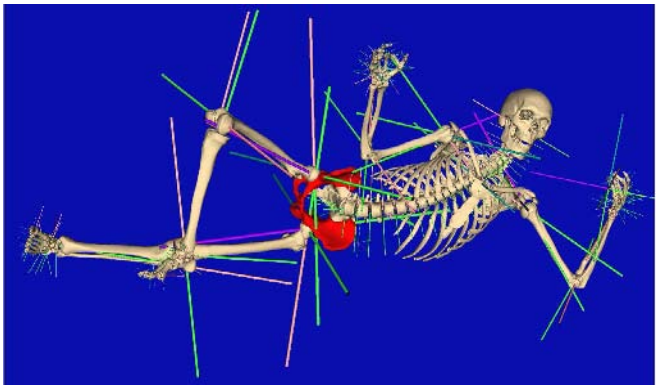

Fig. 3. Whole body Structure with all axes. The kinematic structure is made up of 175 bones, 1.4 Million triangular polygons (stl files), and 194 rotatory degrees of freedom.

placement of axes is based upon knowledge from the literature. Spinal segment limitations in range-of-motion were set first based upon the work of White and Panjabi [14], and then, through iterative monitoring of subsequent motion, were corrected based upon joint congruence and bone segment interaction. The same approach applied to axes of other joints [8, 9, and 10].

Prior work in our lab [4] developed muscle-tendon path models for the extremities using B-Splines with several possible blending functions and three types of control points (bone relative, tendon relative or floating). Most control points were of the bone relative type, representing a rigid constraint or soft tissue pulley point. The floating type provided for sliding along the surface of a bone when within a certain region of a bone surface. Tendon relative points allowed for the origination or connection of one tendon/muscle to another tendon or otherwise dynamically altering surface. Using this same procedure, the major muscles of the back and spine were defined.

This report focuses upon the muscles crossing the index finger metacarpophalangeal (MCP) joint and the knee (see Figs. 4 and 5). For simplicity, we examine the results for

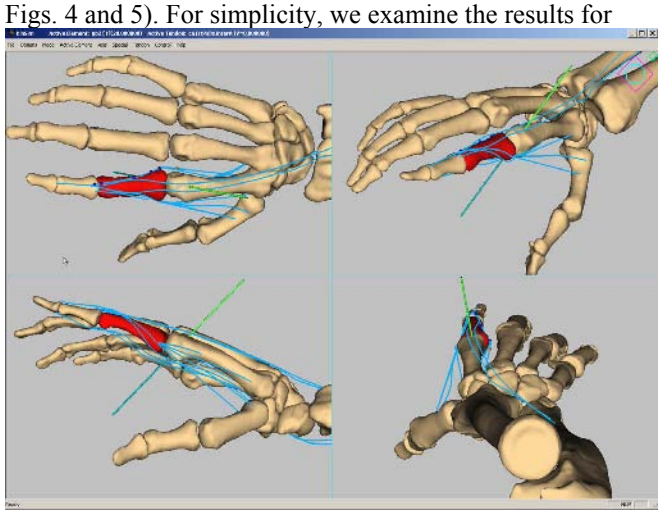

Fig. 4. Four views of the hand simulation including the B-Spline path models for all muscles to the index finger. The path of the First Palmar Interosseous muscle is highlighted by including its B-spline control points and is most in view at the top left.

two muscles: the first palmar interosseous muscle at the Index MCP joint and the sartorius muscle at the knee.

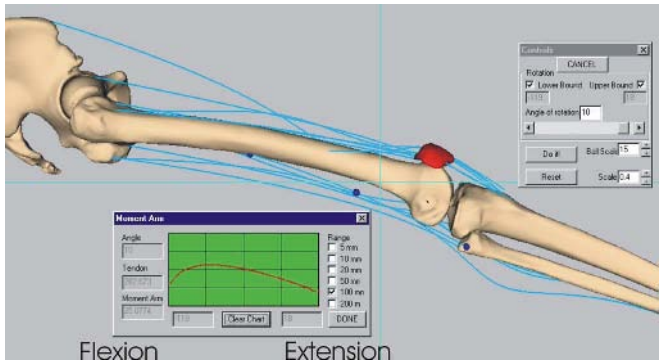

Fig. 5. A lateral view of the right leg from the simulation with the spline path models for all muscles crossing the knee. The biceps femoris short (BFS) is shown with its three control points highlighted and the graph in the bottom center of the view depicts the magnitude of the BFS as it would appear in real-time when rotating the knee from the extended position shown to full flexion.

B. Generation of Moment Arms

The simulation is used interactively to generate moment arms in real-time during user driven joint motion. A given muscles moment arm is displayed (as shown in Fig. 6 for the first palmar interosseous muscle at the index MCP joint) and

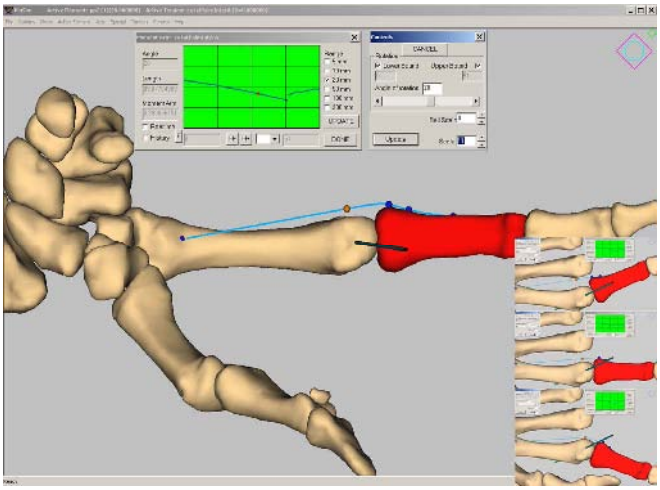

Fig. 6. Volar (palmar) view of the right hand with the third through fifth rays removed for clarity in observing the spline path model and moment arm of the first palmar interosseous muscle as the finger is rotated from radial deviation to ulnar deviation. The bottom right portion of the figure shows the sequence with full radial deviation on the bottom, neutral position in the center and full ulnar deviation above. The magnitude of the moment arm is displayed in the graph at the top of the display. The moment arm is greatest in full ulnar deviation.

saved to an output file. Note in Fig. 6 that the magnitude of the moment arm in this initial model for the muscle increases as the finger rotates from radial to ulnar deviation. Similarly, when performing FE motion at the knee, the moment arm of

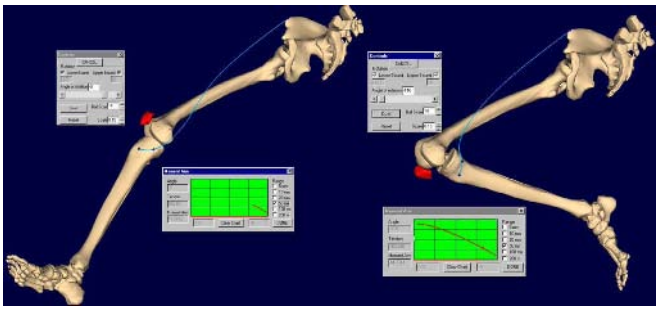

Fig. 7. The moment arm for the sartorius muscle is displayed as the knee is rotated from extension to flexion. It is at a minimum when extended (left) and maximum when flexed.

the sartorius muscle is studied (Fig. 7). The simulation prediction is an increasing moment arm with flexion.

C. Cadaver Experimental Methods

In the experimental portion of the study fresh cadaver arms and legs were acquired through the Texas willed body program. Specimens were dissected through limited incisions but sufficiently to attach nylon cable to finger and knee tendons using previously described methods [1, 2]. All muscles at the knee and all metacarpal phalangeal (MCP) joints in the hand were studied. Muscle excursions, and joint angles (flexion-extension (FE) and ulnar-radial deviation (UR) at the MCP joints; FE and Internal-External rotation (IE) at the knee) were measured. Instantaneous moment arms were determined as the derivative of excursion with respect to angle [1, 6, 7, 12, and 13].

Experimental results are moment arm magnitudes with respect to each rotational degree of freedom studied. Simulation generated moment arms are compared with the experimental results and in all cases studied to date, glaring differences can be attributed to erroneously placed muscle path control points which are corrected with reference to known anatomic constraints supported by other literature or more focused dissection studies. Subtle differences were often diminishes through choice of B-spline blending functions made available in the simulation.

III. Results

The study reported in [5] used the moment arm results to confirm the relative contribution of intrinsic and extrinsic muscles to flexion at the index MCP joint. However, in this report we use the moment arm results for the UR degree of freedom at that joint. The results for all index finger muscles in ulnar-radial motion are displayed in Fig. 8.

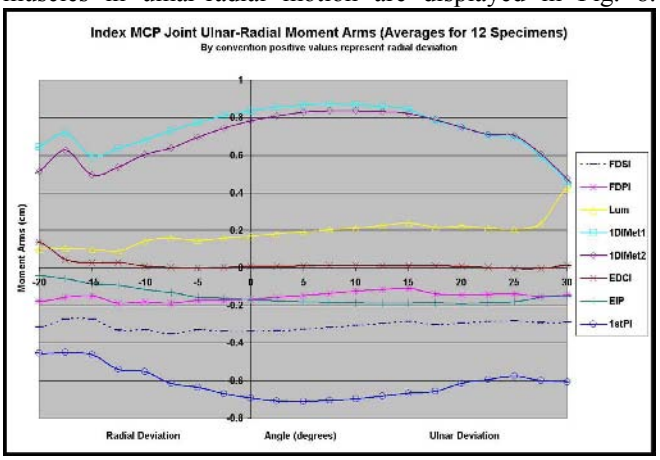

Fig. 8. Moment Arms in Ulnar-Radial deviation rotation at the index metacarpophalangeal joint. Radial deviation is to the left. By arbitrary convention ulnar deviation moment arms are displayed as negative. The moment arm magnitude for first palmar interosseous (1stPI) makes it the most significant ulnar deviator.

The value of the initial, simulation predicted moment arm is inverted to compare in the same sense with the experimental results in Fig. 9. The disagreement between experiment and

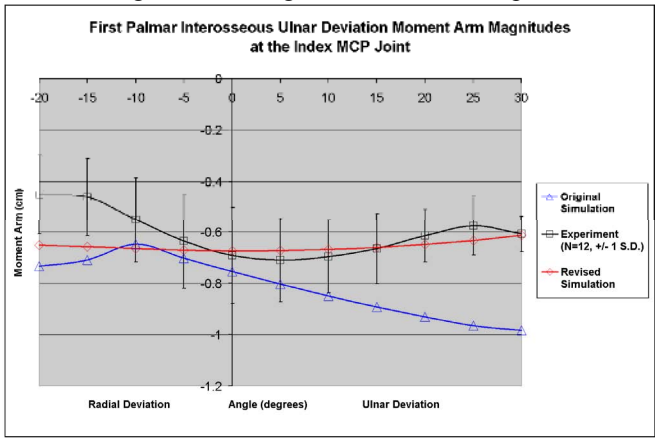

Fig. 9. Comparison of simulation prediction, experimental data and revised simulation moment arms for the first palmar interosseous muscle of the index finger.

simulation prediction implies that the B-Spline model path erroneously moved away from the effective center of

motion. Redefinition of a single B-spline control point, representing a more distinct soft tissue constraint resulted in

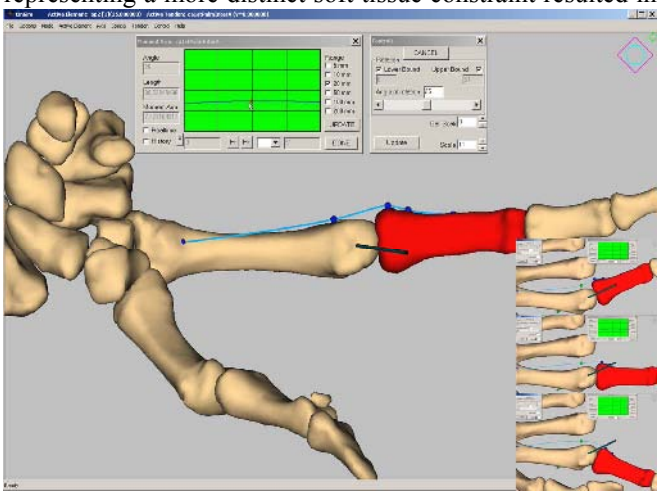

Fig. 10. A simple conversion of a single control point for the B-Spline model of the first palmar interosseous muscle resulted in the generation of a moment arm throughout the ulnar-radial range of motion that closely resembles the experimental results. Compare with Fig. 6 to note the subtle difference in position of the second control point just ulnar to the metacarpal head.

improvement shown in Figs 9 and 10.

Experimental Results for moment arms at the knee are completely defined for Flexion-Extension and Internal-External rotations in [6] and [7]. For flexion extension moment arms the simulation predictions agreed without requiring significant adjustment of muscle model parameters. The Sartorius moment arm depicted in Fig. 7 fell well within the standard deviation of experimental results (Fig. 11).

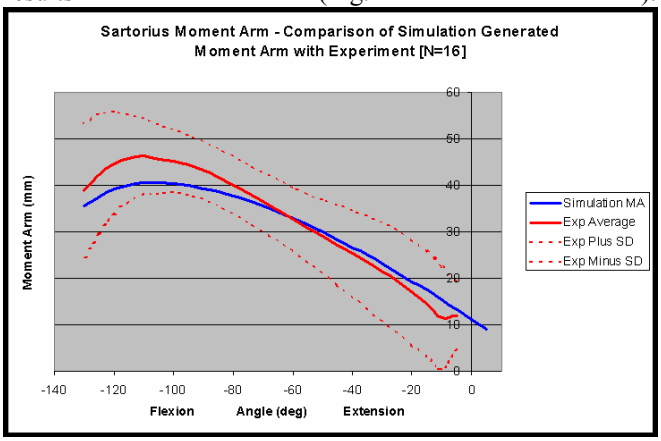

Fig. 11. Simulation predicted moment arm for the Sartorius muscle in knee flexion motion superimposed over experimental results.

IV. Summary and Conclusion

Results reported here cite two representative muscles, one each at the knee and the index MCP joint, and two joint motions, Flexion-extension at the knee and Ulnar-Radial deviation at the index MCP joint. The initial simulation moment arm for the 1stPI in ulnar deviation at the index MCP joint differed from the experimental data with an average residual of 2mm (40%, range of 9 to 68%). This was improved to 0.5mm (10%, range of -5 to 43%) with the single control point correction. For the Sartorius muscle in flexion at the knee no major control point corrections were necessary, and the average residual was 1.25mm (0.05%, range of -34% to 12%). Hence, we conclude that B-spline curve paths are effective models for muscle motion at joints; model parameters can be iteratively adjusted to generate moment arms that agree with experimental data in magnitude and characteristic shape; and the study of muscle moment arms with real-time 3D graphical simulation serves to improve clinical understanding of joint function as well as enhance the research cycle. Though these studies serve to improve muscle models at all joints (recent efforts have helped to clarify the excursion and strain in the pectoralis major muscle at the shoulder [11]), work must continue to verify underlying models of muscles at all joints.

V. References

[1] An, KN, Takahashi, Harrigan, TP, Chao, EY, Determination of Muscle orientations and Moment Arms, J of Biomechanical Engineering 1984, 106: 280-282.

[2] Brand PW, Beach RB, Thompson DE. Relative tension and potential excursion of muscles in the forearm and hand, J Hand Surg 1981; 6:209-219.

[3] Buford, WL, Jr., Andersen, CR, "Definition of the Kinematic Plant for the Human Musculoskeletal System," **Proceedings**, IEEE International Conf. On Systems, Man and Cybernetics, IEEE catalog no. 05CH37706C, Waikoloa, Hawaii, Oct 10-12, 2005, p 1246.

[4] Buford, WL, Jr., Andersen, CR, Elder, KW, Patterson, RM, "Verification of Spline-path Muscle Models for a 3D Simulation of the Extremities," **Proceedings**, ISB, Zurich, Jul 8-13, p 206. 2001.

[5] Buford, WL, Jr., Andersen, CR, Koh, S.,Viegas, SF, Understanding Int-Extrinsic Muscle Function Through Interactive 3D Kinematic Simulation, *J. of Hand Surgery*, Nov; 30a(6):1267-1275, 2005.

[6] Buford, W.L., Jr., Ivey, F.M., Malone, J.D., Patterson, R.M., Peare, G., Nguyen, D., and Stewart, A.A., "Muscle Balance at the Knee-Moment Arms for the Normal Knee and the ACL Minus Knee," *Trans on Rehabilitation Engineering*, 5(4):367-379, Dec 1997.

[7] Buford, W.L., Jr., Ivey, F. M., Nakamura, T., and Patterson, R.M., Nguyen, D., "Internal/External Rotation Moment Arms of Muscles at the Knee - Moment Arms for the Normal Knee and the ACL-Deficient Knee," *The Knee*, 8(4):293-303, October, 2001.

[8] Hollister A, Buford WL, Myers LM, Giurintano DJ, Novick, "The axes of rotation of the thumb carpometacarpal joint," *J Orthop Res*, May;10(3):454-60, 1992.

[9] Hollister A, Giurintano DJ, Buford WL, Myers LM, Novick A, "The axes of rotation of the thumb interphalangeal and metacarpophalangeal joints," *Clin Orthop Relat Res,* Nov; (320):188-93, 1995.

[10] Hollister AM, Jatana S, Singh AK, Sullivan WW, Lupichuk , "The axes of rotation of the knee," *Clin Orthop Relat Res* May ;(290):259-68, 1993.

[11] Jansen, CW, Buford, WL, Jr., Patterson, RM, Gould, LJ, "A Model of Length Increases of the Pectoralis Major Muscle to Provide Rehabilitation Precautions for Patients after Mastectomy," **Proceedings**, IEEE Engineering in Medicine and Biology 27th Annual Conference, Shanghai, China, 1-4 Sep 2005.

[12] Koh, S, Buford, W.L., Jr., Andersen, CR, Viegas, SF, "Intrinsic Muscle Contribution to the Metacarpophalangeal Joint Flexion Moment of the Middle, Ring, and Little Fingers," In Press, *Am J. of Hand Sur.* 2006.

[13] Shah, M.A., Buford, W.L., Jr., Viegas, S.F., "Effects of extensor pollicus longus transposition and extensor indicis proprius transfer to extensor pollicis longus on Thumb Mechanics," *Am J. of Hand Sur.*, 28 (4):661-668, July, 2003.

[14] White, AA, Panjabi, MM, "The Basic Kinematics of the Human Spine - A Review of Past and Current Knowledge," *Spine*. 3(1):12-20, 1978.